nature immunology

CD160 inhibits activation of human CD4+ T cells through interaction with herpesvirus entry mediator

Guifang Cai, Anukanth Anumanthan, Julia A Brown, Edward A Greenfield, Baogong Zhu & Gordon J Freeman

CD160, a glycosylphosphatidylinositol-anchored member of the immunoglobulin superfamily, is expressed on both cytolytic lymphocytes and some unstimulated CD4+ T cells. Here we show that CD160 expression was increased after activation of human CD4+ T cells and that crosslinking CD160 with monoclonal antibody strongly inhibited CD3- and CD28-mediated activation. We found that herpesvirus entry mediator (HVEM) was a ligand of CD160 that acted as a 'bidirectional switch' for T cell activation, producing a positive or negative outcome depending on the engagement of HVEM by CD160 and known HVEM ligands such as B and T lymphocyte attenuator (BTLA) and the T lymphocyte receptor LIGHT. Inhibition of CD4+ T cell activation by HVEM-transfected cells was dependent on CD160 and BTLA; when the cysteine-rich domain 1 of HVEM was deleted, this inhibition was lost, resulting in strong T cell activation. CD160 thus serves as a negative regulator of CD4+ T cell activation through its interaction with HVEM.

The glycosylphosphatidylinositol (GPI)-anchored CD160 protein is expressed mainly on cytolytic cells such as CD8+ T cells, natural killer (NK) T cells and NK cells[1–4]. CD160 has a single immunoglobulin V (IgV)–like domain that is weakly homologous to killer cell immunoglobulin-like receptors, contains six cysteine residues in this IgV domain, and is expressed on the cell surface as a multimer that is tightly linked by disulfide bonds[3]. Classical and nonclassical major histocompatibility complex (MHC) class I molecules bind to CD160 with low affinity[4–7], and this binding might enhance NK and T cell cytolytic activity[5–7].

Because the original monoclonal antibody (mAb) to CD160 (BY55) is a relatively low-affinity IgM subtype[2], we generated new mAbs specific to human CD160 to evaluate its function. Although CD160 is expressed on a few CD4+ T cells, its function on these cells has not been investigated. We found that the new mAbs to CD160 strongly inhibited CD4+ T cell proliferation and cytokine production. This unexpected result led us to search for CD160 ligands other than MHC class I molecules. Here we identify herpesvirus entry mediator (HVEM) as a CD160 ligand by expression cloning and show specific interaction between CD160 and HVEM. We further show that monomeric antibody to CD160 (anti-CD160 Fab) and monoclonal anti-HVEM blocked HVEM-mediated inhibition of T cell activation. Our studies indicate that HVEM is even more 'promiscuous' than previously thought: it interacts with CD160 in addition to binding to the T lymphocyte receptor LIGHT, lymphotoxin-α and BTLA. We also found that CD160 and BTLA bound to cysteine-rich domain 1 (CRD1) of HVEM, but neither CD160 nor BTLA blocked binding of LIGHT to CRD2 and CRD3 of HVEM. Our data collectively show that CD160 functions as an inhibitor of CD4+ T cell activation by interacting with HVEM.

RESULTS

CD160 is expressed on subsets of CD4+ and CD8+ T cells

To investigate the function of CD160, we generated two mAbs to CD160, 5D.10A11 and 5D.8E10, which we characterized as a mouse IgG1 (mIgG1) subtype. We then compared the specificity of 5D.10A11 with that of the original mAb BY55 for CD160 both in cells that were transfected to express CD160 and in responder CD4+ T cell subpopulations. 5D.10A11 bound specifically to human CD160-transfected 300.19 cells at an amount comparable to BY55 (**Fig. 1a** and **Supplementary Fig. 1a** online); experiments with 5D.8E10 produced similar results (data not shown).

To characterize the expression of CD160 in primary human lymphocytes, we stained peripheral blood mononuclear cells (PBMCs) with anti-CD160 (5D.10A11-PC5; **Fig. 1b**). CD160 was expressed on both CD4+ and CD8+ T cells in small amounts (about 8% and about 18% respectively); these results were comparable to staining with BY55 (ref. 2 and **Fig. 1b**). To determine whether expression of CD160 varies with the activation status of CD4+ T cells, we stained purified human CD4+ T cells with antibodies to either the naive or activated form of the cell surface protein CD45 (CD45RA or CD45RO, respectively) in combination with anti-CD160 (5D.10A11; **Fig. 1c**). We found that CD160 was expressed on a considerable subpopulation of memory (CD45RA−CD45RO+) CD4+

Department of Medical Oncology, Dana-Farber Cancer Institute, Department of Medicine, Harvard Medical School, Boston, Massachusetts 02115, USA. Correspondence should be addressed to G.J.F. (gordon_freeman@dfci.harvard.edu).

Received 9 October 2007; accepted 5 December 2007; published online 13 January 2008; corrected after print 16 March 2008; doi:10.1038/ni1554

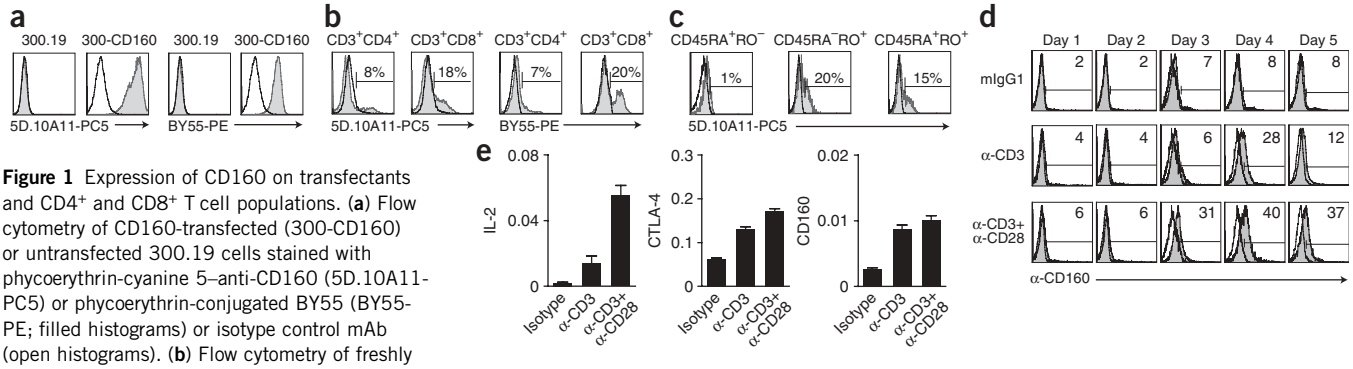

Figure 1 Expression of CD160 on transfectants and CD4+ and CD8+ T cell populations. (**a**) Flow cytometry of CD160-transfected (300-CD160) or untransfected 300.19 cells stained with phycoerythrin-cyanine 5–anti-CD160 (5D.10A11-PC5) or phycoerythrin-conjugated BY55 (BY55-PE; filled histograms) or isotype control mAb (open histograms). (**b**) Flow cytometry of freshly isolated human PBMCs stained with anti-CD160 (5D.10A11-PC5), phycoerythrin-conjugated BY55, fluorescein isothiocyanate–conjugated anti-CD3 or phycoerythrin-indotricarbocyanine–conjugated anti-CD4 or anti-CD8; numbers above bracketed lines indicate percent positive cells among gated $CD3^+CD4^+$ or $CD3^+CD8^+$ cells. (**c**) Flow cytometry of purified $CD4^+$ T cells stained with fluorescein isothiocyanate–conjugated anti-CD45RA, phycoerythrin-conjugated anti-CD45RO and phycoerythrin-cyanine 5–anti-CD160-PC5 (5D.10A11); numbers above bracketed lines indicate percent positive cells among gated $CD45RA^+CD45RO^-$, $CD45RA^-CD45RO^+$ or $CD45RA^+CD45RO^+$ cells. (**d**) Flow cytometry of purified $CD4^+$ T cells stimulated with latex beads (1 μg/ml of anti-CD3 with or without 0.5 μg/ml of anti-CD28) at a ratio of 1:1 (beads/cells) in 24-well plates; cells were collected on days 1–5 and stained with anti-CD160 before analysis. Numbers above bracketed lines indicate percent positive cells. (**e**) Quantitative RT-PCR of total RNA extracted from the cells in **d** at 16 h after activation; values are relative to *GAPDH* mRNA ('housekeeping gene'). α, anti-. Data are representative of six (**a**,**b**) or three (**c**–**e**) experiments.

T cells and recently activated ($CD45RA^+CD45RO^+$) $CD4^+$ T cells but was barely detectable on naive T cells ($CD45RA^+CD45RO^-$), which suggested that CD160 is induced after T cell activation.

To examine further the expression of CD160 after activation, we stimulated purified $CD4^+$ T cells for 1–5 d with anti-CD3 or anti-CD3 plus anti-CD28 (**Fig. 1d**). Expression of CD160 was upregulated on day 3 and peaked on day 4 after activation. Further studies with quantitative RT-PCR (qRT-PCR) showed that like mRNA encoding interleukin 2 (*IL2*) and the T cell inhibitory receptor CTLA-4 (*CTLA-4*), *CD160* mRNA was upregulated 16 h after activation (**Fig. 1e**), which demonstrated that *CD160* expression is induced during $CD4^+$ T cell activation.

Crosslinking of CD160 prevents $CD4^+$ T cell activation

Studies have shown that CD160 enhances the cytolytic activity of $CD8^+$ T cells and NK cells. Expression of CD160 is lower on $CD4^+$ T cells than on $CD8^+$ T cells, and the function of CD160 in $CD4^+$ T cell activation is unclear. To examine the function of CD160 in $CD4^+$ T cell activation, we stimulated purified $CD4^+$ T cells with latex beads coated with various concentrations of mAb to CD160, together with anti-CD3 or anti-CD3 plus anti-CD28. We kept the amount of protein on the beads constant by adding isotype control mIgG1. Unexpectedly, crosslinking of CD160 on $CD4^+$ T cells strongly inhibited T cell proliferation mediated by anti-CD3 or anti-CD3 plus anti-CD28 in a dose-dependent way (**Fig. 2a**). Crosslinking of CD160 did not lead to an increase in cell death, as judged by propidium iodide staining (**Supplementary Fig. 1b**).

The paradox of low CD160 expression but global suppression on crosslinking led us to investigate this issue more closely. Sorted $CD160^-CD4^+$ T cells were more resistant to CD160-mediated suppression; however, the addition of a fivefold higher concentration of anti-CD160 induced a degree of suppression similar to that noted for total $CD4^+$ T cells (**Fig. 2b**). This observation suggested that low CD160 expression or activation-induced CD160 expression is sufficient to mediate inhibition. We examined the effect of CD160 crosslinking on cytokine production by cytokine bead assay. The concentrations of both T helper type 1 (T_H1) cytokines (IL-2, tumor necrosis factor (TNF) and interferon-γ (IFN-γ)) and T_H2 cytokines (IL-4, IL-5, IL-10 and IL-13) at 16 h after activation were progressively diminished by the addition of increasing concentrations of anti-CD160 (**Fig. 2c**). IL-1β, IL-8 and IL-6 were also downregulated, although the reduction in IL-8 required higher concentrations of anti-CD160.

We used microarray analysis to search for suppressive mediators that might be induced by CD160 crosslinking. We extracted total RNA from $CD4^+$ T cells stimulated with anti-CD3 plus anti-CD28 with or without anti-CD160 and from unstimulated $CD4^+$ T cells (mIgG1 isotype control) at various time points after activation (4, 16 and 48 h). Initial analysis of *IL2* mRNA by qRT-PCR showed that *IL2* was maximally upregulated by anti-CD3 plus anti-CD28 at 16 h after activation and was reduced to background by engagement of CD160 (**Fig. 2d**). We therefore used RNA extracted at 16 h after activation in a microarray analysis (Human U-133 plus 2.0, Affymetrix) to compare gene expression in cells stimulated with anti-CD3 plus anti-CD28 with or without anti-CD160 and in unstimulated cells (isotype control). No known suppressive genes (*TGFB1*, *IL10*, *PDCD1*, *CD274*, *PDCD1LG2* and *CTLA4*) were upregulated by CD160 engagement. Most interleukin mRNAs upregulated by stimulation with anti-CD3 plus anti-CD28 were suppressed by crosslinking of CD160 (**Fig. 2e**). Among these mRNAs, we confirmed reductions in *IL2*, *IL6* and *IL17A* mRNA by qRT-PCR (data not shown); *IL2RA* (CD25) mRNA was also suppressed by crosslinking of CD160, although expression of *IL4R* was upregulated. mRNA expression of another interleukin receptor, *IL7R*, was downregulated by anti-CD3 plus anti-CD28 but, after CD160 crosslinking, was restored to the amount in the isotype control.

CD28 costimulation can enhance T cell activation by promoting glucose metabolism[8]. Several small-nutrient transporter gene family mRNAs that were upregulated by anti-CD3 plus anti-CD28 were inhibited by anti-CD160 (**Fig. 2f**), which suggested that suppression of small-nutrient transporter mRNA expression might form part of the CD160-mediated pathway. To determine whether inhibition of IL-2 production is a key factor in CD160-mediated suppression, we added exogenous IL-2 to the culture. Inhibition of T cell activation by CD160 was not 'rescued' by the addition of exogenous IL-2 (**Fig. 2g**), however, which indicated that mechanisms other than IL-2 reduction are important in CD160-mediated inhibition of $CD4^+$ T cells.

Finally, because it has been demonstrated that GPI-anchored CD59 can enhance T cell activation through the recruitment of tyrosine

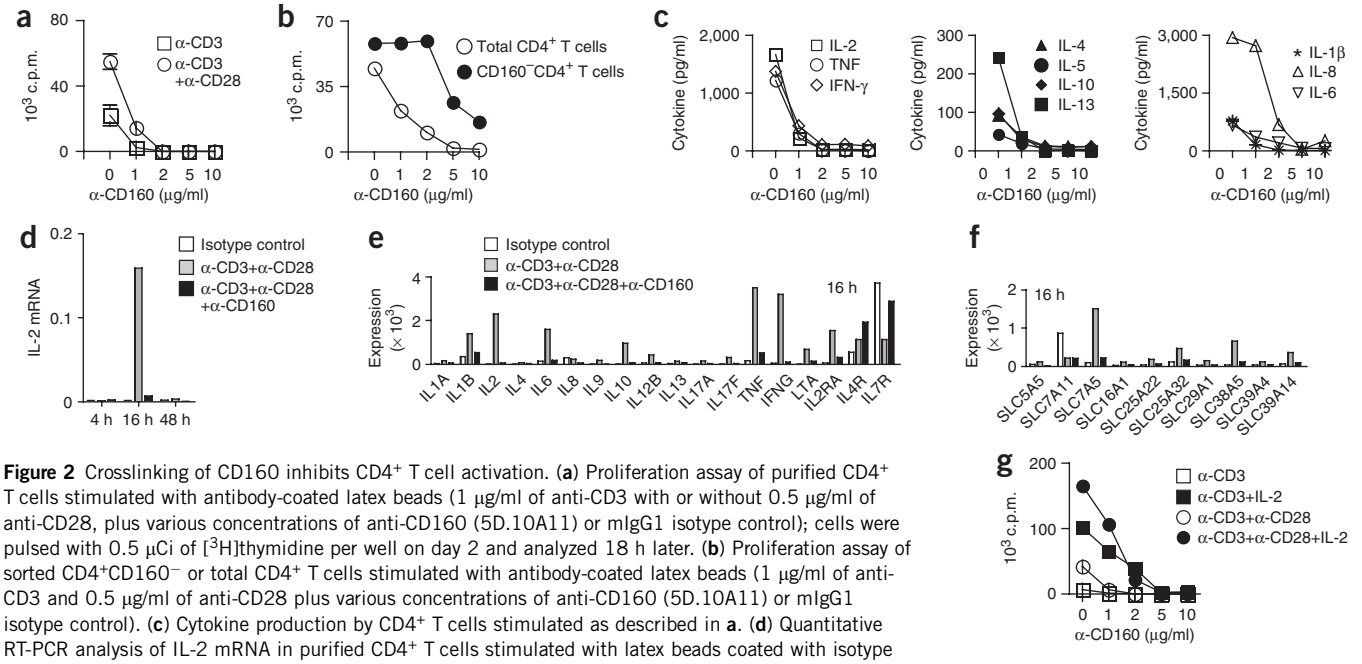

Figure 2 Crosslinking of CD160 inhibits CD4+ T cell activation. (**a**) Proliferation assay of purified CD4+ T cells stimulated with antibody-coated latex beads (1 μg/ml of anti-CD3 with or without 0.5 μg/ml of anti-CD28, plus various concentrations of anti-CD160 (5D.10A11) or mIgG1 isotype control); cells were pulsed with 0.5 μCi of [3H]thymidine per well on day 2 and analyzed 18 h later. (**b**) Proliferation assay of sorted CD4+CD160− or total CD4+ T cells stimulated with antibody-coated latex beads (1 μg/ml of anti-CD3 and 0.5 μg/ml of anti-CD28 plus various concentrations of anti-CD160 (5D.10A11) or mIgG1 isotype control). (**c**) Cytokine production by CD4+ T cells stimulated as described in **a**. (**d**) Quantitative RT-PCR analysis of IL-2 mRNA in purified CD4+ T cells stimulated with latex beads coated with isotype control mAb alone or with anti-CD3 (1 μg/ml), anti-CD28 (0.5 μg/ml) and either anti-CD160 (10 μg/ml) or an equal amount of mIgG1 isotype control, for RNA extracted at 4, 16 or 48 h; expression is relative to that *GAPDH* mRNA. (**e**,**f**) Microarray analysis of mRNA expression in the cells in **d** 16 h after stimulation; cytokines (**e**) and small-nutrient transporters (**f**) are grouped together. (**g**) Proliferation assay of CD4+ T cells treated with 1,000 U/ml of human IL-2 and latex beads coated with antibody, as described in **a**. Data are representative of twenty (**a**), three (**b**), four (**c**,**d**,**g**) or two (**e**,**f**) experiments.

kinases[9], we examined the effect of CD160 crosslinking on tyrosine phosphorylation in CD4+ T cells. Activation mediated by anti-CD3 plus anti-CD28 resulted in enhanced tyrosine phosphorylation of several proteins relative to that of unstimulated cells treated with the mIgG1 isotype control (**Fig. 3a**). In contrast, crosslinking of CD160 reduced tyrosine phosphorylation of the four main proteins induced by anti-CD3 plus anti-CD28 stimulation (**Fig. 3a**, arrowheads). CD3ζ is a small protein that is tyrosine-phosphorylated on T cell activation[10]; we therefore immunoprecipitated CD3ζ and analyzed it by immunoblot with horseradish peroxidase (HRP)–conjugated anti-phosphotyrosine. We found that anti-CD160 crosslinking suppressed the phosphorylation of CD3ζ (**Fig. 3b**), indicating that CD3ζ is one of the targets of the anti-CD160 mediated inhibition of CD4+ T cell activation.

Cloning HVEM as a CD160 ligand

Although MHC class I molecules can bind CD160 with weak affinity[4–7], we found that a mAb to MHC class I molecules (W6/32) did not reverse the inhibitory effect of anti-CD160 on CD4+ T cell activation (data not shown), which suggested that another receptor is involved in this pathway. To identify an additional receptor for CD160, we generated an expression construct in which the extracellular domain of CD160 was linked to human IgG4 Fc (CD160-Ig). After SDS-PAGE, staining with Ponceau S showed that CD160-Ig migrated as a principal band of about 52 kDa (**Fig. 4a**), and immunoblot analysis indicated that anti-CD160 (5D.10A11) bound specifically to the CD160-Ig fusion protein (**Fig. 4b**). Amino-terminal protein sequencing of the 52-kDa band identified the initial nine amino acids as I*ITSSASQ (where '*' is most likely to be a glycosylated residue or cysteine), thus confirming the fusion protein as human CD160-Ig (INITSSASQ; ref. 3).

To identify a cell population expressing a CD160 ligand, we stained human PBMCs with biotin-conjugated CD160-Ig. We found that CD160-Ig bound to CD20+ B cells and CD14+ monocytes but showed minimal binding to CD4+ T cells, CD8+ T cells or NK cells (**Fig. 4c**). Notably, CD160-Ig did not universally stain PBMCs, as would be expected if it were binding to MHC class I (**Fig. 4c**). This observation suggests that binding of CD160 to MHC class I molecules may be too weak to be detected by a soluble CD160-Ig protein. Anti–MHC class I (W6/32) did not block the binding of CD160-Ig to B cells, which suggested that the fusion protein was binding to a high-affinity ligand other than MHC class I (data not shown).

We thus used a B cell cDNA library[11] expressed in transformed African green monkey kidney COS cells to clone the CD160 ligand by immunoselection with CD160-Ig (ref. 12). After three rounds of immunoselection and enrichment, we sequenced individual cDNAs. Nine of the eleven cDNA clones sequenced encoded human HVEM (*TNFRSF14*), each differing only in the length of the 5′ untranslated region. Notably, no MHC class I cDNAs were identified in this cloning procedure. COS cells transiently transfected with HVEM cDNA showed specific binding to CD160-Ig but not to control CTLA-4–Ig (**Fig. 4d**). Control cells transfected with B7.1 showed specific binding to CTLA-4–Ig but not to CD160-Ig. These results collectively suggested that HVEM is a ligand of CD160. To compare the expression of HVEM and the CD160 ligand, we used mAb to HVEM to stain PBMCs from healthy donors. Anti-HVEM showed a staining pattern (**Fig. 4e**) similar to that of CD160-Ig staining (**Fig. 4c**): some B cells and CD14+CD3− monocytes were positive for HVEM, but CD4+ and CD8+ T cells expressed little HVEM.

Specific binding between CD160 and HVEM

To examine further the specificity of the association between CD160 and HVEM, we examined the direct binding of CD160 to HVEM by using purified proteins in an enzyme-linked immunoassay (ELISA). Plate-bound HVEM-mIgG2a demonstrated dose-dependent binding to both CD160-Ig and mAb to HVEM but no binding to a control fusion protein of CTLA-4 and human IgG4 (CTLA-4–Ig; **Fig. 5a**). To

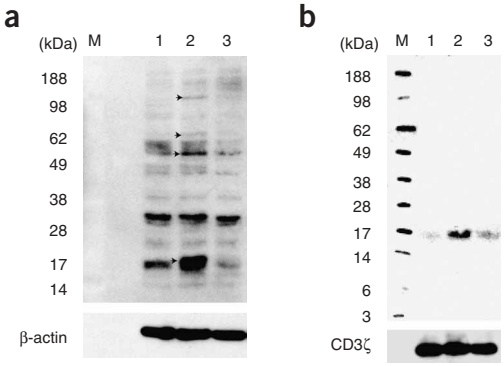

Figure 3 Engagement of CD160 inhibits the tyrosine phosphorylation of several proteins induced by anti-CD3 and anti-CD28. (**a**) Immunoblot analysis of total lysates of purified CD4$^+$ T cells stimulated with latex beads coated with mIgG1 alone (lane 1) or with anti-CD3 and anti-CD28 plus equal amounts of either mIgG1 (lane 2) or anti-CD160 (lane 3), then crosslinked for 4 min at 37 °C with goat anti-mIgG (20 μg/ml), analyzed with HRP-conjugated mAb to phosphorylated tyrosine. Arrows indicate increases in tyrosine phosphorylation induced by anti-CD3 and anti-CD28. M, molecular size markers. Bottom, membrane stripped and blotted with anti-β-actin as a loading control. (**b**) Immunoprecipitation and immunoblot analysis of total cell lysates from cells stimulated as described in **a**; lysates were precleared with protein A and G beads and immunoprecipitated with anti-CD3ζ and protein A and G beads, and the beads were then washed, eluted and analyzed by immunoblot with HRP-conjugated mAb to phosphorylated tyrosine. Bottom, membrane stripped and blotted with anti-CD3ζ as a loading control. Data are representative of three (**a**) or four (**b**) experiments.

confirm that finding further, we generated stable transfectants of 300.19 cells expressing HVEM. Untransfected 300.19 cells did not express either HVEM or CD160, and stable transfectants had considerable expression of HVEM or CD160 after introduction of the respective gene (**Fig. 5b**). 'Titration' of the binding of CD160-Ig, BTLA-Ig and LIGHT-decahistidine (decahis) to HVEM-transfected 300.19 cells showed that BTLA and CD160 had similar affinities for HVEM, but LIGHT had a higher affinity (**Supplementary Fig. 2a–c** online). LIGHT, BTLA and lymphotoxin-α have been shown to bind specifically to HVEM, whose extracellular region comprises four CRDs[13,14]. LIGHT and lymphotoxin-α binding has been mapped to CRD2 and CRD3 of HVEM[15], whereas BTLA binding is localized to CRD1 (refs. 16,17).

To map the CD160-binding site on HVEM, we constructed a mutant HVEM lacking the amino-terminal CRD1 domain (HVEMΔCRD1). Phenotyping of HVEM- and HVEMΔCRD1-transfected 300.19 cells with polyclonal anti-HVEM showed similar expression in the cells. We found that CD160-Ig bound to 300-HVEM cells, as did BTLA-Ig and LIGHT-decahis, but none of the proteins bound to untransfected 300.19 cells (**Fig. 5c**). In addition, CD160, BTLA and LIGHT did not bind to each other (**Supplementary Fig. 2d**). Deletion of CRD1 of HVEM completely abolished both CD160-Ig and BTLA-Ig binding but had no effect on LIGHT binding, which indicated that CRD1 is essential for association with both BTLA and CD160 but not with LIGHT. This finding shows that CD160 and BTLA bind to the same domain of HVEM.

Further confirming the specificity of binding, preincubation of CD160-Ig with anti-CD160 (5D.10A11) reduced the binding of CD160-Ig to HVEM-transfected 300.19 cells almost to background (**Fig. 5d**). Conversely, HVEM-Ig bound specifically to CD160-transfected 300.19 cells and not to untransfected 300.19 cells (**Fig. 5e**). Preincubation of HVEM-Ig with anti-HVEM moderately inhibited the binding of HVEM-Ig to CD160-transfected 300.19 cells. These results collectively show that CD160 and HVEM interact specifically with an affinity sufficient for detection using immunoglobulin fusion proteins and that both CD160 and BTLA bind to the CRD1 domain of HVEM. In addition, we found that a fusion protein of mouse CD160 and mIgG2a (mCD160-Ig) specifically bound to 300.19 transfectants expressing mouse HVEM (mHVEM; **Fig. 5f**). The human CD160, BTLA and LIGHT fusion proteins also bound to mHVEM-transfected 300.19 cells, indicating these interactions are conserved across species (data not shown).

To test whether CD160, BTLA and LIGHT compete or cooperate for binding to HVEM, we preincubated HVEM-transfected 300.19 cells with CD160-Ig, BTLA-Ig or LIGHT-decahis, followed by BTLA-Ig, CD160-Ig or LIGHT-decahis (**Fig. 5g–i**). We found that CD160-Ig

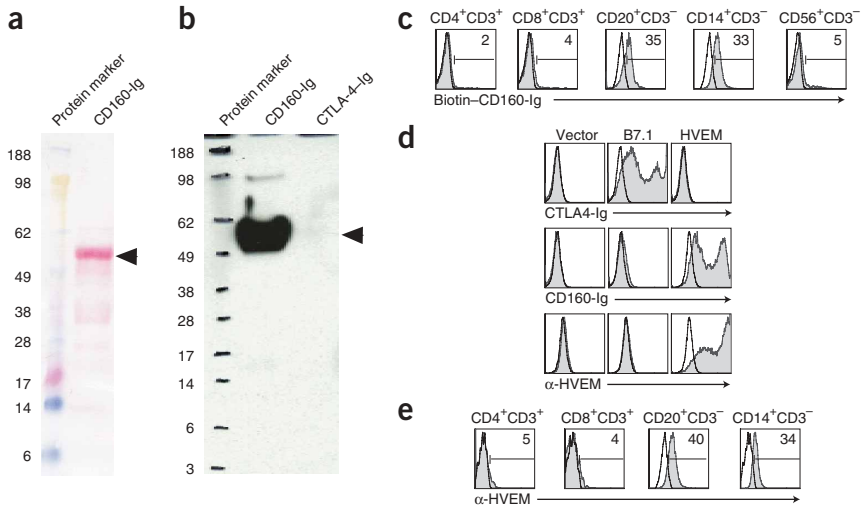

Figure 4 Cloning of HVEM as a CD160 ligand. (**a**,**b**) SDS-PAGE of purified CD160-Ig (5 μg protein per lane) stained with Ponceau S (**a**) or analyzed by immunoblot with anti-CD160 (5D.10A11, 1 μg/ml) and detected with HRP-conjugated goat anti–mouse IgG1 (**b**). (**c**) Flow cytometry of PBMCs stained with biotin-conjugated CD160-Ig (filled histograms) or isotype control mIgG1-biotin, followed by streptavidin–phycoerythrin-indotricarbocyanine (open histograms) and lineage-specific markers (CD3 and CD4, CD8, CD20, CD14 or CD56). Cells were gated on cells positive for lineage-specific markers. Numbers above bracketed lines indicate percent positive cells. (**d**) Flow cytometry of COS cells transfected with plasmids encoding HVEM or B7.1 cDNA, or vector alone, collected on day 3 and stained with CD160-Ig, CTLA-4–Ig or mAb to HVEM (filled histograms) or control human IgG4 fusion protein (open histograms). (**e**) Flow cytometry of PBMCs stained with allophycocyanin-conjugated anti-HVEM and lineage-specific markers (CD3 and CD4, CD8, CD20 or CD14). Cells were gated on cells positive for lineage-specific markers; numbers above bracketed lines indicate percent HVEM$^+$ cells. Data are representative of two (**a**,**b**), three (**c**,**e**) or five (**d**) experiments.

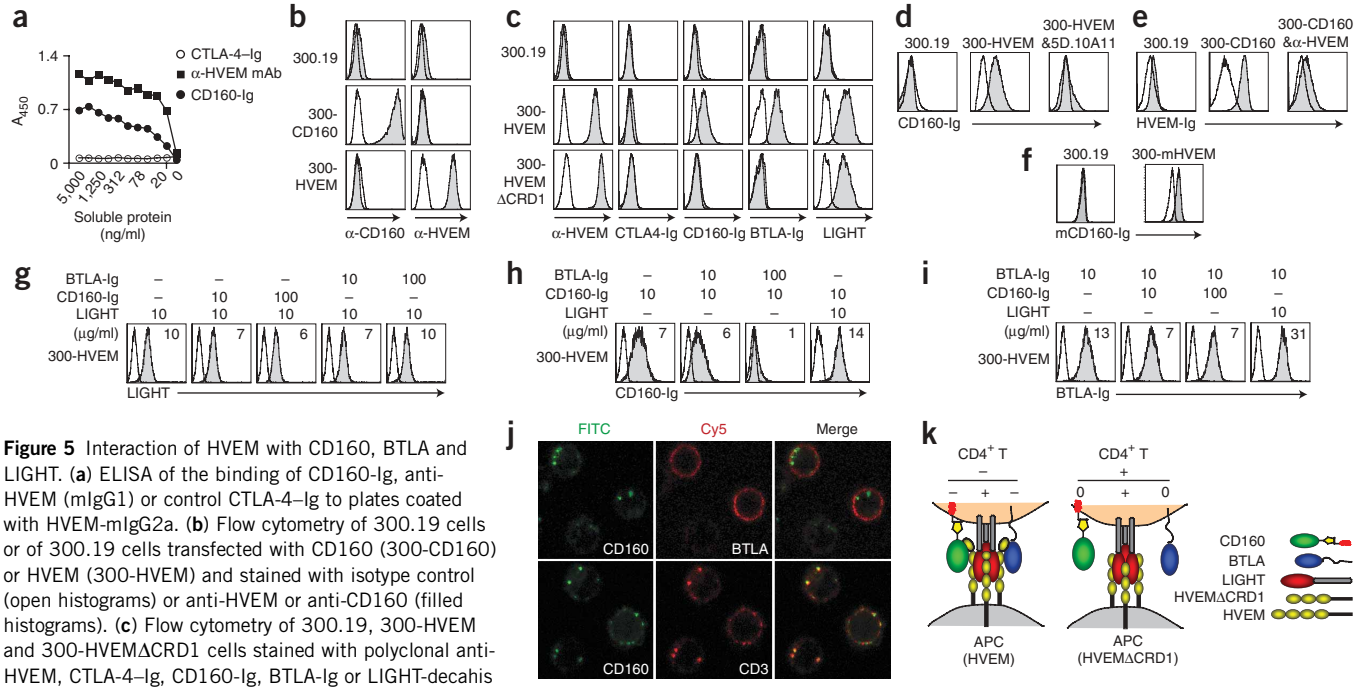

Figure 5 Interaction of HVEM with CD160, BTLA and LIGHT. (**a**) ELISA of the binding of CD160-Ig, anti-HVEM (mIgG1) or control CTLA-4–Ig to plates coated with HVEM-mIgG2a. (**b**) Flow cytometry of 300.19 cells or of 300.19 cells transfected with CD160 (300-CD160) or HVEM (300-HVEM) and stained with isotype control (open histograms) or anti-HVEM or anti-CD160 (filled histograms). (**c**) Flow cytometry of 300.19, 300-HVEM and 300-HVEMΔCRD1 cells stained with polyclonal anti-HVEM, CTLA-4–Ig, CD160-Ig, BTLA-Ig or LIGHT-decahis (filled), or with isotype control (open). (**d**) Flow cytometry of 300.19 or 300-HVEM cells stained with isotype control (open) or with CD160-Ig or CD160-Ig preincubated with anti-CD160 (filled). (**e**) Flow cytometry of 300.19 or 300-CD160 cells stained with isotype control (open), or with HVEM-mIgG2a or HVEM-mIgG2a pre-incubated with anti-HVEM (filled). (**f**) Flow cytometry of 300.19 or 300-mHVEM cells stained with isotype control (open) or mCD160-Ig (filled). (**g–i**) Flow cytometry of 300-HVEM cells stained with 10 μg/ml of isotype control (open), LIGHT-decahis, CD160-Ig or BTLA-Ig, alone or in various combinations (filled), and detected with phycoerythrin-conjugated anti-LIGHT (for LIGHT; **g**), anti–human IgG (for CD160-Ig; **h**) or anti-mIgG2a (for BTLA-Ig; **i**). Numbers in plots indicate mean fluorescence intensity. (**j**) Confocal microscopy of stimulated CD4+ T cells stained with anti-CD160 (green) and anti-BTLA (red) or with anti-CD160 (green) and anti-CD3 (red). Right, merge of fluorescein isothiocyanate (FITC) and indodicarbocyanine (Cy5) images; colocalization is yellow. Original magnification, ×600. (**k**) Interaction of HVEM or HVEMΔCRD1 with CD160, BTLA and LIGHT. APC, antigen-presenting cell. Data are representative of three (**a**,**d**,**e**,**j**), six (**b**,**c**), five (**f**) or four (**g–i**) experiments.

and BTLA-Ig had little effect on the binding of LIGHT to HVEM (**Fig. 5g**). By contrast, LIGHT modestly enhanced the binding of CD160-Ig and BTLA-Ig to HVEM-transfected 300.19 cells, as indicated by a twofold increase in mean fluorescence intensity (**Fig. 5h**,**i**). When we tested BTLA and CD160 for cross-blocking, 10 μg/ml of BTLA-Ig slightly decreased and 100 μg/ml of BTLA-Ig almost completely blocked the binding of CD160-Ig to HVEM (**Fig. 5h**). CD160-Ig had less effect on the binding of BTLA-Ig to HVEM: 10 μg/ml and 100 μg/ml of CD160-Ig only slightly decreased the binding of BTLA-Ig to HVEM (**Fig. 5i**). These results suggest that the BTLA- and CD160-binding sites on HVEM overlap, but they do not exclude the possibility that binding of BTLA could result in a conformational change that affects binding of CD160. Confocal microscopy showed that in previously activated CD4+ T cells, CD160 was present in discrete patches (probably lipid rafts) and did not localize together with BTLA (**Fig. 5j**). A proportion of CD3 did localize together with CD160. These results enable us to propose a model of the interaction of HVEM with its ligands (**Fig. 5k** and discussed below).

HVEM-CD160 and HVEM-BTLA inhibit CD4+ T cell activation

Preliminary experiments showed that activated CD4+ T cells could express all three HVEM ligands: CD160, BTLA and LIGHT (**Fig. 1d** and **Supplementary Fig. 3** online). To examine further the effects of engaging the HVEM-CD160-BTLA pathway, we stimulated CD4+ T cells with latex beads coated with anti-CD3 plus anti-CD28 and engaged the HVEM-CD160-BTLA pathway with anti-CD160, anti-BTLA or HVEM-Ig. We measured proliferation by dilution of the cytosolic dye CFSE (**Fig. 6a**). We found that 36% of the positive control cells stimulated with anti-CD3 plus anti-CD28 divided by day 3. Engagement by anti-CD160, anti-BTLA or HVEM-Ig strongly inhibited CD4+ T cell division induced by anti-CD3 plus anti-CD28 such that only 0–6% of cells divided. By day 5, 93% of the positive control cells had divided. Engagement by anti-CD160, anti-BTLA or HVEM-Ig strongly inhibited the CD4+ T cell cycling induced by 0.1 μg/ml of anti-CD3 plus anti-CD28. The stronger signal provided by 1 μg/ml of anti-CD3 plus anti-CD28 was slightly inhibited by anti-CD160 or HVEM-Ig but not by anti-BTLA. These data indicate that the negative signal delivered through anti-CD160, anti-BTLA or HVEM-Ig can inhibit moderate but not strong signals delivered by T cell antigen receptor and CD28.

Conversely, we examined the effects of blocking the HVEM-CD160-BTLA pathway during an antigen-specific memory T cell response *in vitro*. Tetanus toxoid–specific proliferation and IFN-γ production were augmented when HVEM engagement was blocked with soluble monomeric anti-CD160 Fab, anti-BTLA or anti-HVEM (**Fig. 6b**). Blockade of HVEM had a stronger enhancing effect on IFN-γ production than did blockade of CD160 or BTLA alone. We noted similar enhancement of IFN-γ production by anti-CD160 Fab, anti-BTLA or anti-HVEM in an alloresponse (**Fig. 6c**). These results suggest that both CD160 and BTLA contribute to HVEM-mediated inhibition of T cell responses.

The function of HVEM in humans has been studied less intensively and the effect of human HVEM transfectants on T cell activation

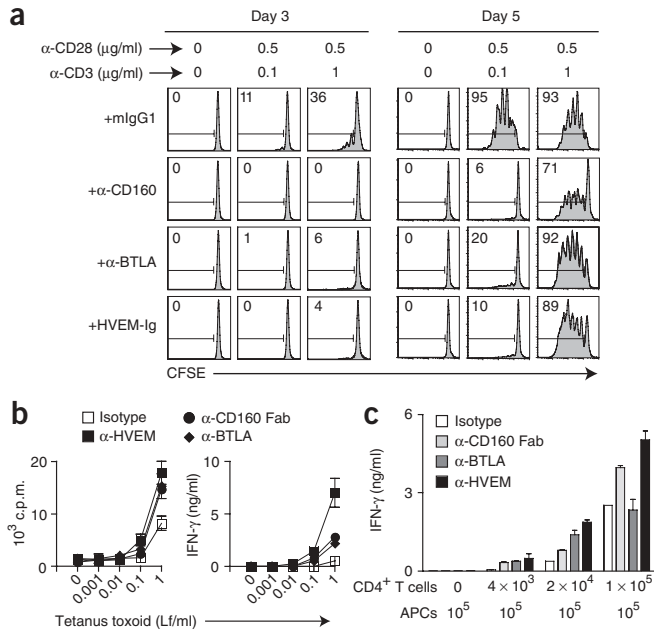

Figure 6 Both CD160 and BTLA inhibit CD4+ T cell activation. (**a**) Proliferation assay of CFSE-labeled CD4+ T cells stimulated with latex beads coated with isotype control mAb or a combination of anti-CD3 (0.1 or 1 μg/ml), anti-CD28 (0.5 μg/ml), and anti-CD160 (5D.10A11), anti-BTLA or HVEM-Ig (10 μg/ml), then collected on days 3 and 5, stained with phycoerythrin-conjugated anti-CD4 and analyzed by flow cytometry for CFSE dilution. Data are CFSE single-parameter histograms gated on CD4+ T cells. Numbers above bracketed lines indicate percent cells that have divided at least once. (**b**) Proliferation and IFN-γ production assays of PBMCs stimulated with tetanus toxoid in the presence of anti–CD160 Fab, anti-BTLA, anti-HVEM or isotype control (each at 10 μg/ml). Supernatants were collected on day 5 for measurement of IFN-γ by ELISA (right); cells were then pulsed with [3H]thymidine and proliferation was measured 18 h later (left). (**c**) ELISA of IFN-γ in supernatants of CD4+ T cells stimulated with irradiated (3,500 rads) allogeneic PBMCs with mIgG1 (isotype control), anti-CD160 Fab, anti-BTLA or anti-HVEM (each at 10 μg/ml) added to the cultures, measured 7 d after stimulation. Data are representative of five (**a**,**b**) or three (**c**) experiments and are the mean ± s.d. of triplicate wells.

has not been published. To explore further the function of the HVEM-CD160 pathway in CD4+ T cell activation, we generated different lines of artificial antigen-presenting cells (NIH-3T3 cells) expressing HVEM or the HVEMΔCRD1 mutant along with the MHC class II molecule DR7 or DR7 plus B7.1 (called DR7, DR7-B7.1, DR7-HVEM, DR7-B7.1-HVEM and DR7-B7.1-HVEMΔCRD1 cells here). We found similar expression of DR7 in all five transfectants, similar expression of B7.1 in DR7-B7.1, DR7-B7.1-HVEM and DR7-B7.1-HVEMΔCRD1 transfectants, and similar expression of HVEM in DR7-HVEM, DR7-B7.1-HVEM and DR7-B7.1-HVEMΔCRD1 transfectants (**Fig. 7a**).

We used a DR7 alloantigen–specific CD4+ T cell line, 2C1, with moderate expression of CD160 (**Fig. 7b**) to determine the functional effect of HVEM binding to CD160. As expected, DR7 transfectants modestly and DR7-B7.1 transfectants strongly stimulated T cell proliferation and cytokine production (**Fig. 7c**). Expression of HVEM on the transfected cells led to potent inhibition of T cell proliferation and cytokine production (**Fig. 7c**). There was a decrease of more than 90% in proliferation between DR7-HVEM and DR7 transfectants, and an 80% decrease in proliferation between DR7-B7.1-HVEM and DR7-B7.1 transfectants. To determine the contribution of CD160 and BTLA to HVEM-mediated inhibition, we used a monomeric anti-CD160 Fab that acts as a blocking reagent, monoclonal anti-BTLA or monoclonal anti-HVEM. All three antibodies equally reversed the HVEM-mediated inhibition of T cell proliferation noted with DR7-B7.1-HVEM transfectants (**Fig. 7d**). All three antibodies enhanced IL-13 and IFN-γ production, and anti-HVEM was more effective than anti-CD160 Fab or anti-BTLA. These results show that both CD160 and BTLA contribute to the HVEM-mediated inhibition of T cell activation.

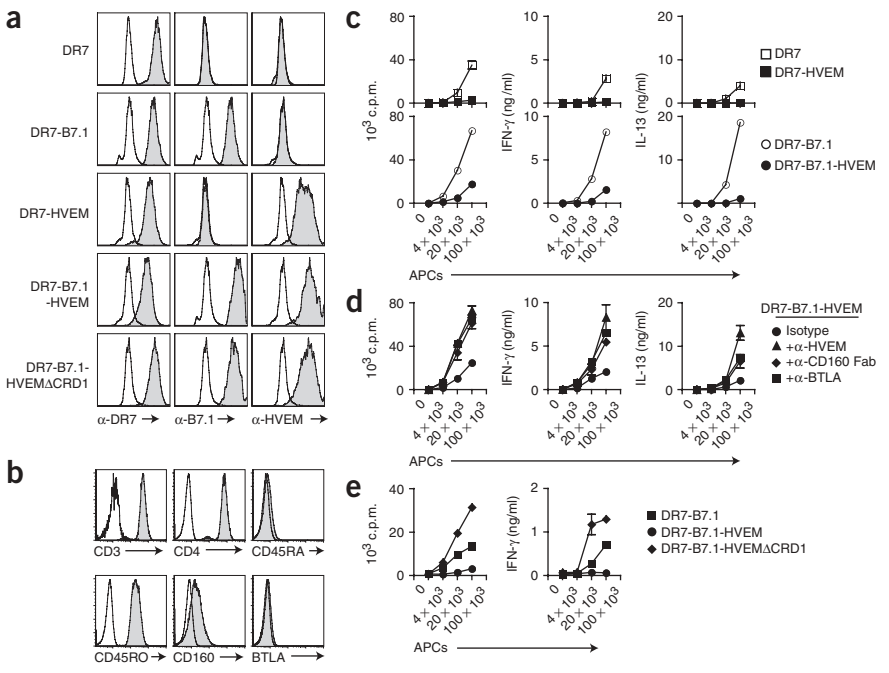

Figure 7 HVEM-transfected NIH-3T3 cells inhibit CD4+ T cell activation and inhibition can be reversed by anti–CD160 Fab or by deletion of CRD1 of HVEM. (**a**) Flow cytometry of NIH-3T3 cells transfected with DR7, B7.1, HVEM or HVEMΔCRD1 and stained with isotype control (open histograms), anti-DR7, anti-B7.1 or anti-HVEM (filled histograms). (**b**) Flow cytometry of resting 2C1 T cells stained with mAbs (to molecules below plots). (**c**) Proliferation and cytokine production assays of the DR7 alloantigen–specific T cell line 2C1 after incubation with NIH-3T3 transfectants; supernatants were collected on day 3 for the cytokine assay and wells were then pulsed with [3H]thymidine and proliferation was measured 18 h later. (**d**) Proliferation and cytokine production assays of the T cell line 2C1 after incubation with DR7-B7.1-HVEM transfectants in the presence of anti-HVEM, anti-CD160 Fab, anti-BTLA or isotype control Fab (10 μg/ml). (**e**) Proliferation and cytokine production by CD4+ T cells stimulated with NIH-3T3 transfectants. Data are representative of three (**a**,**b**) or four (**c**–**e**) experiments (data in **c**,**d** are from the same experiment and represent the mean ± s.d. of triplicate wells).

Because CRD1 of HVEM is required for both CD160 and BTLA but not LIGHT binding, we tested whether deletion of CRD1 would eliminate the suppressive function of HVEM. We compared the capacity of DR7-B7.1 transfectants expressing either HVEM or HVEMΔCRD1 to regulate $CD4^+$ T cell activation in an alloresponse. Unexpectedly, DR7-B7.1-HVEMΔCRD1 transfectants enhanced T cell activation and IFN-γ production even more strongly than did DR7-B7.1 transfectants (**Fig. 7e**). As before, DR7-B7.1-HVEM transfectants inhibited T cell activation. Because deletion of CRD1 of HVEM abolishes CD160 and BTLA binding and mutational analysis[22] indicates that CRD2 and CRD3 are important for binding to LIGHT and lymphotoxin-α, these data suggest that the inhibitory effect of CD160 or BTLA binding to HVEM dominates over the stimulatory effect of LIGHT or lymphotoxin-α binding to HVEM. These data demonstrate that HVEM is an important functional ligand of CD160. Binding of HVEM to CD160 delivers a negative regulatory signal for T cell activation that can be blocked by anti-CD160 Fab, anti-HVEM or deletion of CRD1. Our data collectively show that both CD160 and BTLA contribute to HVEM-mediated inhibition of $CD4^+$ T cell activation, whereas binding of LIGHT to HVEM strongly enhances T cell activation.

DISCUSSION

Using newly generated mAbs to human CD160, we have confirmed that CD160 is expressed on a small percentage of $CD4^+$ T cells and have shown that CD160 is upregulated after $CD4^+$ T cell activation. Crosslinking of CD160 with mAb to CD160 strongly inhibited $CD4^+$ T cell proliferation and cytokine production, thus identifying CD160 as a negative regulator of $CD4^+$ T cell activation. Engagement of CD160 reduced tyrosine phosphorylation of CD3ζ and several other proteins. Microarray analysis showed that CD160 engagement downregulated a broad range of activation-induced genes, including cytokine genes and small-nutrient transporter genes. These results led us to search for CD160 ligands in addition to MHC class I molecules. We identified HVEM as a CD160 ligand by expression cloning and found specific interaction between CD160 and HVEM that resulted in inhibition of T cell activation.

Studies with high-avidity MHC class I tetramers have shown that classical and nonclassical MHC class I molecules bind to CD160 with low affinity[4–7]; however, our CD160-Ig construct did not demonstrate the broad range of binding to cells that would be expected of a universal MHC class I ligand. This observation may be simply a consequence of the lower avidity of a dimeric CD160-Ig fusion protein for cell surface MHC class I than MHC class I tetramers for cell surface CD160. The specific binding of CD160-Ig to B cells and monocytes was not blocked by mAb to MHC class I (W6/32), suggesting that B cells and monocytes express a non-MHC ligand of CD160. Using CD160-Ig, we cloned HVEM from a B cell cDNA library. Staining of PBMCs with mAb to HVEM showed an expression pattern on B cells and monocytes that was similar to the pattern noted for CD160-Ig staining.

Although CD160 is expressed on only about 8% of unstimulated $CD4^+$ T cells, anti-CD160 inhibited most of the T cell population, probably by binding to CD160 expressed after activation. This strong effect of a protein that is weakly expressed on unstimulated cells is similar to that seen for anti-CTLA-4 or anti-PD-1. Indeed, consistent with the expression and function of these other negative regulatory molecules, CD160 has been shown to be upregulated on 'exhausted' T cells[18]. Removal of $CD160^+CD4^+$ T cells from the $CD4^+$ population led to a decrease in inhibition by CD160 engagement; however, high concentrations of anti-CD160 still substantially inhibited T cell activation, probably by binding to CD160 protein expressed after activation. CD160-mediated inhibition was not 'rescued' by exogenous IL-2, which indicated that mechanisms other than IL-2 reduction are important in CD160-mediated $CD4^+$ T cell inhibition.

The mechanism whereby a GPI-anchored protein such as CD160 engages signaling pathways is poorly understood. Studies of GPI-anchored proteins such as CD59, CD90 and CD48 have demonstrated their localization to lipid rafts and modulation of tyrosine kinase activity[9,19]. Phosphotyrosine immunoblot analysis showed that crosslinking of CD160 modulated tyrosine kinase activity with reduced tyrosine phosphorylation of several substrates, particularly CD3ζ. In contrast to BTLA, engagement of CD160 did not induce phosphorylation of the tyrosine phosphatases SHP-1 or SHP-2 (data not shown). CD160 and BTLA might act coordinately in HVEM-mediated inhibition, whereby CD160 modulates the signaling complexes that translocate to lipid rafts and BTLA recruits tyrosine phosphatases[20].

HVEM serves as a bidirectional switch for T cell activation, producing a positive or negative outcome depending on the ligands engaged[21]. Our data have identified CD160 as a HVEM ligand in addition to BTLA, LIGHT and lymphotoxin-α. LIGHT and lymphotoxin-α are members of the TNF superfamily with a trimeric structure, whereas CD160 and BTLA comprise a single immunoglobulin-like domain[3,20]. The HVEM-binding site on LIGHT has been mapped to CRD2 and CRD3 (ref. 15), whereas the binding sites for BTLA, herpes simplex virus glycoprotein D (gD)[22] and CD160 (as shown here) are present in CRD1. The LIGHT-HVEM interaction consists of a LIGHT trimer with an HVEM molecule bound at the interface between each pair of LIGHT monomers, thereby making a 3:3 complex[14]. In this arrangement, the CRD1 of HVEM overhangs the top of the LIGHT molecule and would be accessible for interaction with CD160 or BTLA. Mutagenesis of HVEM has shown that the BTLA- and gD-binding sites are opposite to the LIGHT-binding site[16]. Our cross-blocking studies with CD160 and BTLA indicated that their binding sites on the CRD1 domain of HVEM overlap to some extent, and our colocalization experiments showed that CD160 and BTLA do not associate before interacting with HVEM. Light-scattering analysis has shown that BTLA and HVEM form a 1:1 complex[16]. A soluble HVEM molecule can bind a soluble BTLA molecule and a LIGHT molecule simultaneously[23]. Our binding experiments with HVEM-expressing cells suggested that HVEM can form a complex at the cell surface with BTLA and LIGHT or with CD160 and LIGHT. Indeed, association of LIGHT with HVEM did not block either CD160 or BTLA binding but led to a twofold increase in the mean fluorescence intensity of CD160 or BTLA binding. This observation suggests that a fully formed complex might contain nine molecules: three of HVEM, three of LIGHT, and three in total of BTLA and/or CD160.

HVEM binding to LIGHT on T cells is reported to stimulate T cell activation[24–26], but we found that binding of HVEM to BTLA or CD160 inhibited T cell activation. HVEM-knockout mice have higher T cell activation[27], indicating that the inhibitory function of HVEM is the essential, nonredundant function of HVEM, despite the tenfold higher affinity of HVEM for LIGHT (11 nM) than for BTLA (112 nM; ref. 22). This dominant inhibitory function of HVEM has also been seen in studies with mouse[17] and human (as shown here) $CD4^+$ T cells stimulated with antigen-presenting cells transfected with mouse or human HVEM, respectively. In our experiments, HVEM strongly inhibited T cell responses despite the coexpression of LIGHT with CD160 and BTLA on activated human T cells. Because trimeric HVEM bound both CD160 and BTLA at the same time and blockade

of either BTLA or CD160 reversed the HVEM-mediated inhibition, CD160 and BTLA may act coordinately in HVEM-mediated inhibition. Comparing the T cell responses of CD160 and/or BTLA knockout mice may shed light on this issue.

Our experiments with antigen-presenting cells transfected with HVEMΔCRD1 and HVEM offer insight into the function of HVEM when presented *in trans* to T cells potentially expressing CD160, BTLA and/or LIGHT. Whereas transfectants expressing HVEM inhibited T cell responses, those expressing HVEMΔCRD1 enhanced T cell responses. These results suggest that CRD1 is essential for the delivery of an inhibitory signal and that the inhibitory interaction of HVEM with CD160 and/or BTLA dominates over a stimulatory interaction with LIGHT. When the binding site on HVEM for the inhibitory receptors was eliminated (HVEMΔCRD1), engagement of LIGHT alone led to a potent stimulatory signal. The herpes simplex virus gD protein achieves a similar result by binding to CRD1 of HVEM and blocking the interaction with BTLA. Because the binding sites for BTLA and CD160 overlap, it is likely that CD160 binding is also blocked. Indeed, it has been shown that DNA vaccines expressing an antigen in gD strongly enhance immune responses *in vivo*[28]. During a T cell response, the outcome probably depends on expression of the negative receptors (CD160 and BTLA) relative to the positive receptor (LIGHT). Indeed, studies have shown that constitutive expression of LIGHT results in tissue destruction and autoimmune-like disease syndromes[29], confirming the 'bidirectional' function of HVEM. Expression of HVEM in humans has been reported in placental syncytiotrophoblasts, amnion epithelial cells[30] and umbilical vein endothelial cells[31], which suggests that the interaction of HVEM with CD160 and BTLA might have an important role in regulating tolerance during pregnancy. In addition, $CD160^+CD4^+$ T cells might be involved in inflammatory responses in skin[32].

In summary, we have shown here that CD160 is a ligand of HVEM and that the CD160-HVEM interaction inhibits $CD4^+$ T cell activation. HVEM acts as a bidirectional switch for T cell activation whereby the outcome depends on the ligands engaged[21]. The functional consequence of binding HVEM can be manipulated through genetic modification of the CRD1 region of HVEM. The contribution of each HVEM ligand to the regulation of human immune responses and the best way to manipulate this pathway therapeutically are issues to be investigated.

METHODS

Human subjects. Peripheral venous blood was obtained from normal donors after informed consent under institutional review board approval from the Dana-Farber Cancer Institute.

Antibodies. Mouse mAbs to human CD160 were made by immunizing mice with CD160-Ig and screening hybridoma supernatants on CD160-transfected 300.19 and Chinese hamster ovary cells. Both 5D.10A11 and 5D.8E10 are mouse IgG1 and show specific binding by FACS to CD160-transfected cell lines (300.19, CHO and COS) but not to untransfected cells. We prepared 5D.10A11 Fab and mIgG1 (MOPC-31) Fab with an ImmunoPure IgG1 Fab and Fab_2 preparation kit (Pierce Biotechnology).

CD160-phycoerythrin (BY55-PE; BY55, IgM) was from Immunotech. Goat anti-mouse IgG (1010-09), goat $F(ab')_2$ anti-human IgG (1032-09), goat anti-mIgG2a (1080-09) and goat anti-mIgG1 (1070-09) were from Southern Biotech. Mouse fluorescein isothiocyanate–conjugated anti–goat immunoglobulin (205095108) was from Jackson Immunotech. Anti-DR7 IgM (biotinylated mAb; BIH0108) was from One Lambda. Monoclonal anti-HVEM (94801), polyclonal goat anti-HVEM (AF356), mouse anti–human LIGHT (115520), and recombinant human LIGHT-decahis (664-LI/CF) were from R&D Systems. Human HVEM-Ig (mIgG2a Fc; 531-820) was from Ancell. Anti–human BTLA was from eBioscience. Flow cytometry–staining antibodies to CD3, CD4, CD8, CD14, CD20, CD56, CD45RA, CD45RO, CD69 and CD25 were from BD Biosciences. HRP-conjugated mAb to phosphorylated tyrosine (4G10) was from Upstate.

Fusion proteins and HVEM mutants. CD160-Ig comprised the complete extracellular domain of CD160 fused to the hinge-CH2-CH3 domains of human IgG4 (mutated to reduce FcR binding). The CD160 extracellular domain was amplified by PCR (primers, **Supplementary Table 1** online), digested with *Hin*dIII and *Bgl*II, and ligated into a *Hin*dIII- and *Bcl*I-digested pNRDSH plasmid containing the hinge-CH2-CH3 domains of human IgG4. All restriction endonucleases were from New England Biolabs. The control CTLA-4–Ig comprised the extracellular domain of CTLA-4 linked to the same human IgG4. CD160-Ig was produced in stably transfected NSO cells and was purified from conditioned medium with protein A–sepharose 4B.

Human BTLA-mIgG2a and the mCD160-mIgG2a construct were made by In-Fusion assembly[33]. The BTLA or mCD160 extracellular domain and the hinge-CH2, CH3 of mIgG2a (mutated to reduce FcR binding) were amplified with overlapping primer pairs. The two PCR products were fused in an expression vector by an In-Fusion reaction (Clontech) and confirmed by sequencing. The construct was made linear with *Mlu*I, was electroporated into CHO DG44 cells, was selected by methotrexate resistance, and was cloned as single cells. BTLA-Ig or mC160-Ig was purified from the cell supernatant of the highest producer clone by protein G– or A–sepharose 4B.

The CRD1 domain comprising amino acids 42–75 was deleted from a human HVEM cDNA in pCDM8 in a way analogous to that described for a mouse CRD1 deletion mutant[17]. The amino-terminal end and the carboxy-terminal region of HVEM were amplified by PCR with overlapping primer pairs. The DNAs were incubated with an *Hin*dIII- and *Bsp*EI-digested HVEM plasmid, were joined by an In-Fusion reaction (Clontech), were transformed in *Escherichia coli* cells and were sequenced for confirmation.

Cytokine ELISA, cytokine bead assay, and fusion protein binding ELISA. IL-10, IL-13 and IFN-γ in culture supernatants were assayed by ELISA with mAb to human IL-10 (554497, 554499), IL-13 (554570, 555054; both BD Biosciences) or IFN-γ (2G1, M701B; Endogen) in accordance with the manufacturer's instructions. IL-1β, IL-2, IL-4, IL-5, IL-6, IL-8, IL-10, IL-13, IFN-γ and TNF were determined with a cytokine bead assay kit (BD Biosciences). For measurement of the binding of immunoglobulin fusion proteins, ELISA plates were coated with 5 μg/ml of HVEM-mIgG2a fusion protein and then blocked. Serial dilutions of CD160-Ig, CTLA-4–Ig or monoclonal anti-HVEM were added, and the plates were incubated for 30 min and then washed. Binding was detected by incubation with HRP-conjugated anti–human IgG (for CD160-Ig or CTLA-4–Ig) or anti-mIgG1 (1:10,000, for anti-HVEM), coupled with development with TMB substrate and measurement of absorbance at 450 nm (A_{450}).

Cloning of a CD160 ligand with CD160-Ig. A B cell cDNA library in the pCDM8 expression vector[34] was transiently transfected into COS cells by GeneJuice (Novagen). COS cells were collected 44 h after transfection and were incubated with 10 μg/ml of CD160-Ig. Cells were washed and then $CD160\text{-}Ig^+$ cells were enriched by 'panning' on plates coated with Fab_2 goat anti–human IgG. Plasmid was purified and reintroduced into *E. coli* by electroporation. Plasmids were transfected into COS cells by spheroplast fusion with polyethylene glycol, and $CD160\text{-}Ig^+$ cells were immunoselected as described above. After three rounds of immunoselection, plasmids were individually purified, transfected into COS cells with GeneJuice, and stained with 10 μg/ml of CD160-Ig on day 3.

Transfected cell lines. NIH-3T3 cells transfected with human DR7 were maintained in medium[35] containing 45% (vol/vol) DMEM, 45% (vol/vol) F12, 10% (vol/vol) FCS, 2 mM GlutaMAX and 200 μg/ml of G418 (drug selection for DR7; ref. 35; all from Invitrogen). Human HVEM or HVEMΔCRD1 in pCDM8 and a plasmid encoding puromycin resistance were introduced by electroporation into NIH-3T3 cells expressing DR7 or DR7-B7.1. Positive cells were selected with 1 μg/ml of puromycin and then were sorted with mAb to HVEM and subcloned to obtain stable transfectants.

We stably transfected 300.19 cells with human CD160, BTLA, HVEM or HVEMΔCRD1 or with mouse HVEM or CD160 by electroporation, sorted the cells by using specific antibodies and then cloned them. For fusion protein–binding assays, 300.19 transfectants were incubated for 15 min on ice with 10 μg/ml of fusion protein, washed and then incubated for 10 min at 25 °C with phycoerythrin-conjugated goat anti–human IgG (CD160-Ig binding assay), goat anti-mIgG2a (HVEM-Ig binding assay) or mouse anti–human LIGHT (LIGHT-binding assay). For blocking, the fusion protein was incubated for 30 min on ice with a specific or isotype control mAb before being added to 300.19 transfectants. The cells were then washed and analyzed immediately by flow cytometry.

PBMC isolation and tetanus toxoid stimulation. PBMCs were purified by density gradient centrifugation using Ficoll/Hypaque (Pharmacia Biotech). Cells (2×10^5 PBMCs per well) in 5% (vol/vol) human AB serum medium (RPMI-1640, 2 mM GlutaMAX, 1,000 U/ml of penicillin, 10 μg/ml of streptomycin, 10 mM HEPES, pH 7.2, 1 mM sodium pyruvate and 1% (vol/vol) nonessential amino acids; all from Mediatech) were stimulated with various concentrations of tetanus toxoid (University of Massachusetts Medical Center) combined with 10 μg/ml of anti-CD160 Fab (5D.10A11) or mIgG1 Fab as indicated. On day 5 after activation, 100 μl of supernatant was collected for the cytokine assay, cells were pulsed with 0.5 μCi of [^{3}H]thymidine per well and the counts per minute (c.p.m.) were measured.

CD4$^+$ T cell purification and activation with coated latex beads. CD4$^+$ T cells were purified from freshly isolated PBMCs by depletion of non-CD4$^+$ T cells by magnetic beads using a T cell isolation kit II (Miltenyi); purity was judged to be over 90% by flow cytometry. Latex beads (5 μm in diameter, 4%; Invitrogen) were coated with various concentrations of anti-CD3 (UCHT1; BD Biosciences), anti-CD28 (MAB342; R&D), and/or various concentrations of anti-CD160 (5D.10A11 or 5D.8E10) or mIgG1. The amount of protein was kept constant at 11.5 μg/ml by the addition of control mIgG1. Antibodies and beads in PBS were incubated for 1.5 h at 37 °C. Latex beads were washed once with 10% (vol/vol) FCS in RPMI medium and then were blocked for 30 min at 37 °C with 10% (vol/vol) FCS in RPMI medium. Beads were then washed and were added at a 1:1 ratio to 96-well U-bottomed plates containing 5×10^4 T cells per well. At 16 h after stimulation, 100 μl of supernatant was collected and cytokines were assayed. On day 2, cells were pulsed with 0.5 μCi of [^{3}H]thymidine and proliferation was measured 18 h later.

For analysis of T cell division by carboxyfluorescein diacetate succinimidyl diester (CFSE) dilution, CD4$^+$ T cells were washed twice in PBS, were resuspended in PBS at density of 5×10^6 cells per ml, mixed with an equal volume of 1 μM CFSE in PBS, and incubated for 5 min at 25 °C with occasional mixing. Labeling was quenched by the addition of an equal volume of cold FCS. Cells were then centrifuged and were washed twice in 5% human AB serum medium. Cells were plated at a density of 1×10^6 cells per ml in medium in 24-well plates, were stimulated with latex beads coated with mAb or fusion protein and were analyzed after 1–5 d for CFSE dilution by flow cytometry.

2C1 CD4$^+$ T cell clone. The 2C1 allogeneic CD4$^+$ T cell clone specific for DR7 was generated from purified CD4$^+$ T cells (1×10^6 per well) cultured together in 24-well plates with 5×10^5 NIH-3T3 cell DR7-B7.1 transfectants that had been previously treated with 50 μg/ml of mitomycin C. All T cell clones and 3T3 transfectants cultures were prepared in RPMI 1640 medium supplemented with 10% (vol/vol) FCS (Cambrex BioScience), 2 mM GlutaMAX, 1 mM sodium pyruvate, 15 μg/ml of gentamicin (all from Invitrogen), 50 U/ml of penicillin, 50 μg/ml of streptomycin and 10 mM HEPES buffer, pH 7.2 (all from Mediatech). After three stimulations, allogeneic CD4$^+$ T cells were collected by Ficoll gradient, sorted as single cells into 96-well plates and stimulated with 2×10^5 irradiated PBMCs as feeder cells, 5×10^4 DR7-B7.1 transfectants, 50 U/ml of IL-2 (BD Biosciences) and 2 μg/ml of phytohemagglutinin (Sigma Aldrich). The 2C1 T cells were restimulated with DR7-B7.1 transfectants every 4 weeks and their populations were expanded with 50 U/ml of IL-2 every 4 d.

For analysis of the effect of HVEM on T-cell activation, NIH-3T3 transfectants were collected, were washed twice with RPMI media (without antibiotics), were resuspended at a density of 5×10^6 cells per ml, were incubated for 3 h at 37 °C with 50 μg/ml of mitomycin C, were washed twice with medium, and then were plated at various densities in a 200-μl volume per well. The next day, media were removed and 5×10^4 2C1 T cells (**Fig. 7c,d**) or purified CD4$^+$ T cells (**Fig. 7e**) with or without 10 μg/ml of anti-CD160 Fab (5D.10A11), mIgG1 Fab, mAb to BTLA, mAb to HVEM or mIgG1 in 200 μl was added to each well. After 48 h, 100 μl of supernatant were collected for measurement of cytokine production and cells were pulsed with 0.5 μCi [^{3}H]thymidine in 100 μl of medium for measurement of T cell proliferation 18 h later.

Additional methods. Information on immunoblot assay, qRT-PCR, microarray analysis and confocal microscopy is available in the **Supplementary Methods** online.

Note: Supplementary information is available on the Nature Immunology website.

ACKNOWLEDGMENTS

Confocal images were obtained by T. Hickman (Brigham and Women's Confocal Core Facility). Supported by the National Institutes of Health (AI39671 and AI56299 to G.J.F.).

AUTHOR CONTRIBUTIONS

G.C. designed and did the experiments, analyzed the data and wrote the paper; A.A. prepared CD160-Ig and provided some of the initial ideas; J.A.B. prepared 2C1 T cells; E.A.G. generated mAbs to CD160; B.Z. prepared fusion protein and expression constructs; and G.J.F. planned and supervised the project, designed constructs and wrote the paper.

COMPETING INTERESTS STATEMENT

The authors declare competing financial interests: details accompany the full-text HTML version of the paper at http://www.nature.com/natureimmunology/.

Published online at http://www.nature.com/natureimmunology
Reprints and permissions information is available online at http://npg.nature.com/reprintsandpermissions

1. Bensussan, A. *et al.* BY55 monoclonal antibody delineates within human cord blood and bone marrow lymphocytes distinct cell subsets mediating cytotoxic activity. *Proc. Natl. Acad. Sci. USA* **91**, 9136–9140 (1994).
2. Maiza, H. *et al.* A novel 80-kD cell surface structure identifies human circulating lymphocytes with natural killer activity. *J. Exp. Med.* **178**, 1121–1126 (1993).
3. Anumanthan, A. *et al.* Cloning of BY55, a novel Ig superfamily member expressed on NK cells, CTL, and intestinal intraepithelial lymphocytes. *J. Immunol.* **161**, 2780–2790 (1998).
4. Maeda, M. *et al.* Murine CD160, Ig-like receptor on NK cells and NKT cells, recognizes classical and nonclassical MHC class I and regulates NK cell activation. *J. Immunol.* **175**, 4426–4432 (2005).
5. Agrawal, S. *et al.* Cutting edge: MHC class I triggering by a novel cell surface ligand costimulates proliferation of activated human T cells. *J. Immunol.* **162**, 1223–1226 (1999).
6. Barakonyi, A. *et al.* Cutting edge: engagement of CD160 by its HLA-C physiological ligand triggers a unique cytokine profile secretion in the cytotoxic peripheral blood NK cell subset. *J. Immunol.* **173**, 5349–5354 (2004).
7. Le Bouteiller, P. *et al.* Engagement of CD160 receptor by HLA-C is a triggering mechanism used by circulating natural killer (NK) cells to mediate cytotoxicity. *Proc. Natl. Acad. Sci. USA* **99**, 16963–16968 (2002).
8. Frauwirth, K.A. *et al.* The CD28 signaling pathway regulates glucose metabolism. *Immunity* **16**, 769–777 (2002).
9. Stefanova, I., Horejsi, V., Ansotegui, I.J., Knapp, W. & Stockinger, H. GPI-anchored cell-surface molecules complexed to protein tyrosine kinases. *Science* **254**, 1016–1019 (1991).
10. Baniyash, M., Garcia-Morales, P., Luong, E., Samelson, L.E. & Klausner, R.D. The T cell antigen receptor zeta chain is tyrosine phosphorylated upon activation. *J. Biol. Chem.* **263**, 18225–18230 (1988).
11. Freeman, G.J. *et al.* Murine B7–2, an alternative CTLA-4 counter-receptor that costimulates T cell proliferation and interleukin 2 production. *J. Exp. Med.* **178**, 2185–2192 (1993).
12. Seed, B. & Aruffo, A. Molecular cloning of the CD2 antigen, the T cell erythrocyte receptor, by a rapid immunoselection procedure. *Proc. Natl. Acad. Sci. USA* **84**, 3365–3369 (1987).
13. Montgomery, R.I., Warner, M.S., Lum, B.J. & Spear, P.G. Herpes simplex virus-1 entry into cells mediated by a novel member of the TNF/NGF receptor family. *Cell* **87**, 427–436 (1996).
14. Bodmer, J.L., Schneider, P. & Tschopp, J. The molecular architecture of the TNF superfamily. *Trends Biochem. Sci.* **27**, 19–26 (2002).
15. Sarrias, M.R. *et al.* The three HveA receptor ligands, gD, LT-α and LIGHT bind to distinct sites on HveA. *Mol. Immunol.* **37**, 665–673 (2000).
16. Compaan, D.M. *et al.* Attenuating lymphocyte activity: the crystal structure of the BTLA-HVEM complex. *J. Biol. Chem.* **280**, 39553–39561 (2005).

17. Sedy, J.R. *et al.* B and T lymphocyte attenuator regulates T cell activation through interaction with herpesvirus entry mediator. *Nat. Immunol.* **6**, 90–98 (2005).
18. Wherry, E.J. *et al.* Molecular signature of CD8 T cell exhaustion during chronic viral infection. *Immunity* **27**, 670–684 (2007).
19. Morgan, B.P., van den Berg, C.W., Davies, E.V., Hallett, M.B. & Horejsi, V. Cross-linking of CD59 and of other glycosyl phosphatidylinositol-anchored molecules on neutrophils triggers cell activation via tyrosine kinase. *Eur. J. Immunol.* **23**, 2841–2850 (1993).
20. Watanabe, N. *et al.* BTLA is a lymphocyte inhibitory receptor with similarities to CTLA-4 and PD-1. *Nat. Immunol.* **4**, 670–679 (2003).
21. Murphy, K.M., Nelson, C.A. & Sedy, J.R. Balancing co-stimulation and inhibition with BTLA and HVEM. *Nat. Rev. Immunol.* **6**, 671–681 (2006).
22. Cheung, T.C. *et al.* Evolutionarily divergent herpesviruses modulate T cell activation by targeting the herpesvirus entry mediator cosignaling pathway. *Proc. Natl. Acad. Sci. USA* **102**, 13218–13223 (2005).
23. Gonzalez, L.C. *et al.* A coreceptor interaction between the CD28 and TNF receptor family members B and T lymphocyte attenuator and herpesvirus entry mediator. *Proc. Natl. Acad. Sci. USA* **102**, 1116–1121 (2005).
24. Harrop, J.A. *et al.* Herpesvirus entry mediator ligand (HVEM-L), a novel ligand for HVEM/TR2, stimulates proliferation of T cells and inhibits HT29 cell growth. *J. Biol. Chem.* **273**, 27548–27556 (1998).
25. Tamada, K. *et al.* Modulation of T cell-mediated immunity in tumor and graft-versus-host disease models through the LIGHT co-stimulatory pathway. *Nat. Med.* **6**, 283–289 (2000).
26. Tamada, K. *et al.* LIGHT, a TNF-like molecule, costimulates T cell proliferation and is required for dendritic cell–mediated allogeneic T cell response. *J. Immunol.* **164**, 4105–4110 (2000).
27. Wang, Y. *et al.* The role of herpesvirus entry mediator as a negative regulator of T cell–mediated responses. *J. Clin. Invest.* **115**, 711–717 (2005).
28. Lasaro, M.O., Diniz, M.O., Reyes-Sandoval, A., Ertl, H.C. & Ferreira, L.C. Anti-tumor DNA vaccines based on the expression of human papillomavirus-16 E6/E7 oncoproteins genetically fused with the glycoprotein D from herpes simplex virus-1. *Microbes Infect.* **7**, 1541–1550 (2005).
29. Granger, S.W. & Rickert, S. LIGHT-HVEM signaling and the regulation of T cell–mediated immunity. *Cytokine Growth Factor Rev.* **14**, 289–296 (2003).
30. Gill, R.M., Ni, J. & Hunt, J.S. Differential expression of LIGHT and its receptors in human placental villi and amniochorion membranes. *Am. J. Pathol.* **161**, 2011–2017 (2002).
31. Chang, Y.H., Hsieh, S.L., Chao, Y., Chou, Y.C. & Lin, W.W. Proinflammatory effects of LIGHT through HVEM and LTβR interactions in cultured human umbilical vein endothelial cells. *J. Biomed. Sci.* **12**, 363–375 (2005).
32. Abecassis, S. *et al.* Identification of a novel $CD160^{+}CD4^{+}$ T-lymphocyte subset in the skin: a possible role for CD160 in skin inflammation. *J. Invest. Dermatol.* **127**, 1161–1166 (2007).
33. Zhu, B., Cai, G., Hall, E.O. & Freeman, G.J. In-Fusion assembly: seamless engineering of multidomain fusion proteins, modular vectors, and mutations. *Biotechniques* **43**, 354–359 (2007).
34. Freeman, G.J. *et al.* B7, a new member of the Ig superfamily with unique expression on activated and neoplastic B cells. *J. Immunol.* **143**, 2714–2722 (1989).
35. Boussiotis, V.A., Freeman, G.J., Gray, G., Gribben, J. & Nadler, L.M. B7 but not intercellular adhesion molecule-1 costimulation prevents the induction of human alloantigen-specific tolerance. *J. Exp. Med.* **178**, 1753–1763 (1993).

Corrigendum: CD160 inhibits activation of human CD4+ T cells through interaction with herpesvirus entry mediator

Guifang Cai, Anukanth Anumanthan, Julia A Brown, Edward A Greenfield, Baogong Zhu & Gordon J Freeman

Nat. Immunol. **9, 176–185 (2008); published online 13 January 2008; corrected after print 16 March 2008**

In the version of this article initially published, the citation for Supplementary Figure 2c on page 179 and the citation for Supplementary Figure 3a on page 180 are incorrect. These should be "Supplementary Fig. 2a–c" and "Supplementary Fig. 3," respectively. The errors have been corrected in the HTML and PDF versions of the article.